

# Lawrence Berkeley National Laboratory

## Recent Work

### Title

PROPERTIES OF NEGATIVE K MESONS

### Permalink

<https://escholarship.org/uc/item/0rw262ss>

### Authors

Webb, Francis M.  
Iloff, Edwin L.  
Featherston, Frank H.  
[et al.](#)

### Publication Date

1957-09-01

UNIVERSITY OF  
CALIFORNIA

*Radiation  
Laboratory*

TWO-WEEK LOAN COPY

*This is a Library Circulating Copy  
which may be borrowed for two weeks.  
For a personal retention copy, call  
Tech. Info. Division, Ext. 5545*

BERKELEY, CALIFORNIA

## **DISCLAIMER**

This document was prepared as an account of work sponsored by the United States Government. While this document is believed to contain correct information, neither the United States Government nor any agency thereof, nor the Regents of the University of California, nor any of their employees, makes any warranty, express or implied, or assumes any legal responsibility for the accuracy, completeness, or usefulness of any information, apparatus, product, or process disclosed, or represents that its use would not infringe privately owned rights. Reference herein to any specific commercial product, process, or service by its trade name, trademark, manufacturer, or otherwise, does not necessarily constitute or imply its endorsement, recommendation, or favoring by the United States Government or any agency thereof, or the Regents of the University of California. The views and opinions of authors expressed herein do not necessarily state or reflect those of the United States Government or any agency thereof or the Regents of the University of California.

UCRL-3905

UNIVERSITY OF CALIFORNIA

Radiation Laboratory  
Berkeley, California

Contract No. W-7405-eng-48

PROPERTIES OF NEGATIVE K MESONS

Francis M. Webb, Edwin L. Iloff, Frank H. Featherston, Warren W. Chupp,  
Gerson Goldhaber, and Sulamith Goldhaber

September 1, 1957

Printed for the U. S. Atomic Energy Commission

This report was prepared as an account of Government sponsored work. Neither the United States, nor the Commission, nor any person acting on behalf of the Commission:

- A. Makes any warranty or representation, express or implied, with respect to the accuracy, completeness, or usefulness of the information contained in this report, or that the use of any information, apparatus, method, or process disclosed in this report may not infringe privately owned rights; or
- B. Assumes any liabilities with respect to the use of, or for damages resulting from the use of any information, apparatus, method, or process disclosed in this report.

As used in the above, "person acting on behalf of the Commission" includes any employee or contractor of the Commission to the extent that such employee or contractor prepares, handles or distributes, or provides access to, any information pursuant to his employment or contract with the Commission.

Contents

I. Introduction . . . . .	4
II Measurements on Primary $K^-$ Track . . . . .	6
A. Mean Life . . . . .	6
B. Decay Modes . . . . .	6
C. The $K^-$ -Interaction Cross Section . . . . .	7
1. Interaction with Complex Nuclei . . . . .	
(a) Inelastic Scattering Events and Absorption Events . . . . .	7
(b) Charge-Exchange Scattering Events . . . . .	9
2. Elastic Scattering and Total Cross Section . . . . .	9
3. The $K^-$ -Hydrogen Cross Section . . . . .	11
III $K^-$ -Hydrogen Absorption at Rest . . . . .	11
A. The $\Sigma^-$ - $\Sigma^+$ Mass Difference . . . . .	13
B. The $K^-$ Mass . . . . .	13
IV The $K^-$ -Absorption Stars . . . . .	14
A. The Pion Spectrum . . . . .	15
1. The $\Lambda/\Sigma$ Ratio . . . . .	18
B. Comparison Between Absorption at Rest and in Flight . . . . .	19
C. $K^-$ Absorption Stars as a Source of $\Lambda^0$ Hyperons . . . . .	21
1. Energy Balance . . . . .	21
2. Strangeness Balance . . . . .	24
3. Prong Distribution and Visible Energy Release . . . . .	24
V Observation on $\Sigma$ Hyperons . . . . .	25
Appendix . . . . .	31

PROPERTIES OF NEGATIVE K MESONS

Francis M. Webb, Edwin L. Iloff, Frank H. Featherston, Warren W. Chupp,  
Gerson Goldhaber, and Sulamith Goldhaber

Department of Physics and Radiation Laboratory  
University of California, Berkeley, California

September 1, 1957

ABSTRACT

An analysis of interactions of 420-Mev/c  $K^-$  mesons incident on a nuclear emulsion stack has been carried out. By following  $K^-$  mesons along the track, we obtained information on the interaction of  $K^-$  mesons in flight and at rest. The differential scattering cross section was fitted with diffraction scattering off a black disk with radius  $1.32 \times A^{1/3}$  fermis in agreement with the total reaction cross section. A compilation of  $K^-$ -H elastic scattering and absorption events is presented, giving cross sections of  $\sigma_{KH}$  (scattering) =  $48.4^{+15}_{-11}$  mb and  $\sigma_{KH}$  (absorption) =  $11.4^{+9}_{-5}$  mb. The inelastic scattering of  $K^-$  mesons in complex nuclei has been found to be only 4% of the absorption cross section. The average energy losses in  $K^-$  inelastic scattering events is  $\sim 50\%$  of the incident K energy, in contrast to a 25% loss for  $K^+$  inelastic scattering.

In the course of this work we have observed a number of decays in flight. Combining these with earlier data, we obtain a mean life of  $\tau_{K^-} = 1.3^{+0.4}_{-0.3} \times 10^{-8}$  sec. We have identified some of the secondaries from decays in flight, namely  $2 K_{\pi_2}^-$ ,  $2 K_{\mu_2}^-$ , and  $1 K_{e3}^-$ .

From  $K^-$ -H absorption events we have obtained a  $\Sigma^- - \Sigma^+$  mass difference of  $13.9 \pm 1.8 m_e$  and a value of the  $K^-$  mass of  $966.7 \pm 2.0 m_e$ .

From an analysis of the charged pion spectrum obtained from  $K^-$  interactions at rest, it was possible to calculate the ratio of  $\Lambda$  to  $\Sigma$  hyperons produced in the primary interaction. We find that in the primary  $K^-$  nucleon absorption reaction,  $\Sigma$ -hyperon formation dominates over  $\Lambda$ -hyperon formation. An energy and strangeness balance shows that 70% of the  $K^-$  stars at rest emit a  $\Lambda$  particle. This means that about 60% of the  $\Sigma$  hyperons that are produced are converted to  $\Lambda$  hyperons inside the nucleus in which they were formed.

## PROPERTIES OF NEGATIVE K MESONS<sup>\*†</sup>

Francis M. Webb,<sup>§</sup> Edwin L. Iloff,<sup>\*\*</sup> Frank H. Featherston, Warren W. Chupp,  
Gerson Goldhaber, and Sulamith Goldhaber

Department of Physics and Radiation Laboratory  
University of California, Berkeley, California

September 1, 1957

### I. INTRODUCTION

From the study of the interactions of negative K mesons in photographic emulsion, one can obtain information on both the properties of the  $K^-$  mesons and of the  $\Sigma$  and  $\Lambda$  hyperons produced by the interaction of the  $K^-$  mesons with nuclei.

By following "along the track" of  $K^-$  mesons with an incident momentum of 420 Mev/c, we have been able to obtain information on the interaction of  $K^-$  mesons in flight and at rest.

From interactions in flight, we have obtained the elastic differential cross section, which can be fitted by the diffraction scattering from a black disk of radius  $1.32 \times A^{1/3}$  fermis.

A compilation of the K-H elastic scattering and absorption events in the energy interval  $T_{K^-} = 16$  to 150 Mev has been made from which the value

---

\* Paper delivered by Sulamith Goldhaber at the International Conference on Mesons and Recently Discovered Particles, Padua-Venice September 1957. References include only papers published prior to the time of the meeting.

† The material presented in this paper is based in part on the Doctors' Dissertations of Francis M. Webb, University of California Department of Physics, 1957, and Edwin L. Iloff, University of California Department of Physics, 1957, and on the Master's Dissertation of F. H. Featherston, University of California and United States Naval Postgraduate School, Monterey, California. The work was done under the auspices of the U. S. Atomic Energy Commission.

§ Present address: 3454 Vosberg Street, Pasadena, California.

\*\* Present address: Department of Physics, Iowa State College, Ames, Iowa.



of the  $K^-$ -H scattering cross section of  $48.4^{+15}_{-11}$  mb and the  $K^-$ -H absorption cross section of  $11.4^{+9}_{-5}$  mb were deduced. The inelastic scattering of the  $K^-$  mesons in complex nuclei has been found to be only 4% of the absorption cross section.

A number of decays in flight have been observed, which combined with our earlier data yield a mean life of  $\tau_{K^-} = 1.3^{+0.4}_{-0.3} \times 10^{-8}$  sec.

We have been able to identify several decay modes by analyzing the secondaries from the  $K^-$  decays in flight. We have found two  $K_{\pi_2}^-$ , two  $K_{\mu_2}^-$ , and one  $K_{e_3}^-$ .

We have reevaluated our earlier  $K^-$ -H absorption events at rest, i. e.,  $K^- + H \rightarrow \Sigma^\pm + \pi^\mp$ , and have also included an additional event where the resulting  $\Sigma^+$  decays via the  $\Sigma^+ \rightarrow p + \pi^0$  decay mode. From these events we have obtained a  $\Sigma^- - \Sigma^+$  mass difference of  $13.9 \pm 1.8 m_e$  and a value for the  $K^-$  mass of  $966.7 \pm 2.0 m_e$ .

From an analysis of the charged-pion spectrum obtained from  $K^-$  interactions at rest, it was possible to estimate the ratio of  $\Lambda$  to  $\Sigma$  hyperons produced in the primary interaction. We have assumed throughout this analysis that the absorption process of the  $K^-$  mesons proceeds according to the independent-particle model, i. e., the  $K^-$  is absorbed by a single nucleon. The absorption by two nucleons is estimated to occur in no more than 10% of all interactions. We have assumed two extreme models in order to calculate the modification of the pion spectrum due to the energy dependence of the mean free path of pions in nuclear matter: (a) Uniform absorption of  $K^-$  mesons, and (b) surface absorption of the  $K^-$  mesons. The  $\Lambda/\Sigma$  ratio is sensitive to the radius at which the absorption occurs. We have fitted the experimental spectrum by an intermediate model, the average between the two above-mentioned cases.

A comparison of the pion spectrum for interactions of  $K^-$  mesons in flight with that at rest indicates that absorptions in flight occur most probably at a smaller average absorption radius than those at rest.

From an energy and strangeness balance we find that in approximately 70% of the  $K^-$ -absorption stars at rest, a  $\Lambda^0$  particle is emitted. This, when compared with the  $\Lambda/\Sigma$  production ratio, implies that about 60% of the  $\Sigma$  hyperons that are produced are converted to  $\Lambda$  hyperons on leaving the nucleus in which they were formed.

The experimental data presented in this paper come from our own data (based on 364  $K^-$  stars at rest and 102  $K^-$  stars in flight) and also partly on a compilation prepared by one of us for the Sixth Annual Rochester Conference. <sup>1</sup>

## II. MEASUREMENTS ON THE PRIMARY $K^-$ TRACK

In all the work reported here, we followed the  $K^-$  mesons by "along the track" scanning. In this fashion, both decays in flight and interactions in flight are observed. If the  $K^-$  meson does not undergo either of the above processes, it is followed until it comes to rest, and the absorption stars at rest can thus be found in a completely unbiased fashion.

### A. Mean Life

The ratio of the total proper moderation time to the number of decays in flight gives the mean life of the  $K^-$  meson. In an earlier compilation for a total moderation time of  $12.37 \times 10^{-8}$  sec, 13 decays in flight were found, giving a mean life of  $\tau_{K^-} = 0.95^{+0.36}_{-0.25} \times 10^{-8}$  sec. <sup>2</sup> Subsequently we have observed seven additional decays for a total proper moderation time of  $13.85 \times 10^{-8}$  sec. Combining these two results, we obtain  $\tau_{K^-} = 1.3^{+0.4}_{-0.3} \times 10^{-8}$  sec. This is to be compared to the value of  $\tau_{K^-} = 1.49^{+0.22}_{-0.24} \times 10^{-8}$  sec obtained in a recent counter experiment. <sup>3</sup> The evidence is thus very good that the mean life is the same as that for the  $K^+$  meson. <sup>4</sup>

### B. Decay Modes

A study of the decay modes of  $K^-$  mesons is possible only by examining decays in flight. A  $K^-$  meson when brought to rest is captured into atomic orbits of one of the near-by atoms and is subsequently absorbed by the nucleus. It is therefore more difficult to establish the branching ratio into the various decay modes for  $K^-$  mesons than it has been for  $K^+$  mesons, which decay when brought to rest. From a total of 11 secondaries observed, we have identified five which constitute all secondaries with a dip angle  $\leq 15^\circ$ . We found in this unbiased sample two  $K_{\pi_2^-}$ , two  $K_{\mu_2^-}$ , and one  $K_{e_3^-}$  decay modes. <sup>5</sup> The decay of the negative  $\tau$  mesons has been observed in cloud chamber and bubble chamber experiments. <sup>6</sup> So few secondaries were available for analysis that our only conclusion was that the decay modes of the  $K^-$  meson are not inconsistent with those of the  $K^+$  meson. <sup>7</sup>

### C. The $K^-$ Interaction Cross Section

In the 30.6 meters of path length scanned, we have observed 101 inelastic and absorption interactions in complex nuclei and one hydrogen-absorption event ( $K^- + H \rightarrow \Sigma^\pm + \pi^\mp$ ).<sup>8</sup> Table I gives our result on the mean free path for three energy intervals. The mean free path over the entire energy intervals is  $30.3 \pm 3$  cm, excluding the hydrogen events. This mean free path gives an average reaction cross section in emulsion (Ag, Br, and C, O, and N) of  $707 \pm 70$  mb, and the corresponding nuclear radius is  $R = (1.32 \pm 0.07) \times A^{1/3}$  fermis.

#### 1. Interaction with Complex Nuclei

##### (a) Inelastic Scattering Events and Absorption Events

The inelastic scattering cross section of  $K^-$  mesons is only a small fraction of the  $K^-$  reaction cross section ( $\sim 4\%$ ). In 30.4 meters scanned along the track, we have seen only four inelastic scattering events with energy loss  $\frac{\Delta T}{T} > 10\%$ . The measurement technique used to determine energy losses could reliably detect energy changes equal to or greater than 10%. Although the number of inelastic scatters is small, it is interesting to note that in all cases the incident  $K^-$ -meson loses about one-half its kinetic energy in the collision  $\langle \Delta T/T \rangle = 0.56$  (see Table II). This is of particular interest when compared with  $K^+$  mesons, in which the energy losses are generally smaller ( $\langle \Delta T/T \rangle \simeq 0.25$  for  $K^+$  mesons of 20 to 100 Mev). For  $K^+$  mesons the markedly small energy loss, considered to occur in collisions with single bound nucleons, was ascribed to a repulsive nuclear potential. The large energy loss of the  $K^-$  meson in collisions with bound nucleons may be an indication of an attractive nuclear potential.<sup>9</sup> The present limited statistics do not permit a detailed analysis of this phenomenon.

The majority of the interaction of the  $K^-$  mesons in flight lead to absorption stars giving rise to  $\Sigma$  and  $\Lambda$  hyperons. A detailed discussion of these events is given in Section III.

Table I

Energy distribution of the $K^-$ -meson interactions			
$T_{K^-}$ (Mev)	Path length (meters)	Number of events	Mean free path (cm)
16 to 60	6.73	25	$27 \pm 5.4$
60 to 120	14.49	41	$35 \pm 5.5$
120 to 160	9.39	35	$27 \pm 4.5$
16 to 160 average	30.61	101	$30.3 \pm 3$

Table II

Characteristics of inelastic $K^-$ -meson scattering		
$T_{K^-}$ (Mev)	$\Delta T/T$	$\theta_K$ Lab scattering angle (deg)
38	0.58	56
58	0.62	82
103	0.48	59
138	0.55	103

## (b) Charge-Exchange Scattering Events

Charge-exchange scattering events of  $K^-$  mesons in complex nuclei such as we deal with in emulsion cannot be distinguished from absorption stars with neutral hyperon emission. It is, however, possible to set an upper limit to the ratio of charge-exchange scattering to non-charge-exchange scattering. Interference between the singlet and triplet isotopic spin states in the  $K^-$  scattering interaction leads to an upper limit for the ratio

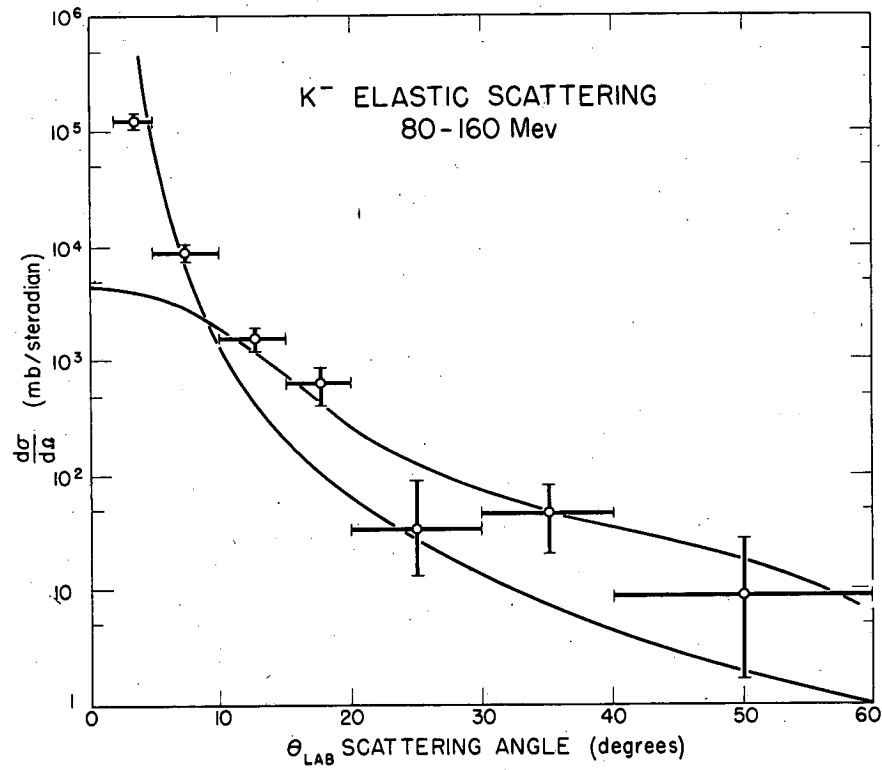
$$\frac{K^- + p \rightarrow \overline{K^0} + n}{(K^- + p \rightarrow K^- + p) + (K^- + n \rightarrow K^- + n)} \leq 2.$$

The charge-exchange scattering of  $K^-$  mesons can therefore be estimated to be  $\lesssim 8\%$  of the reaction cross section.

2. Elastic Scattering and Total Cross Section

The experimental procedure used in determining the elastic cross section consisted of measuring all the space angles of  $K^-$  scattering events for which the projected angles are  $\geq 2^\circ$ . The differential cross section was then computed from these measurements by applying a correction factor, which compensates for the events missed due to the  $1.9^\circ$  cutoff in projected angles. With the  $K^+$  mesons, it was possible to analyze the differential scattering cross section in terms of an optical-model potential.<sup>10,11</sup> For  $K^-$  mesons, the large absorption cross section is evidence for the presence of a large imaginary potential. Conclusions on the sign and magnitude of the real potential are thus more involved in the case discussed here. An exact optical-model calculation similar to the one for  $K^+$  mesons<sup>11</sup> will be carried out shortly.<sup>12</sup>

The data can be fitted by a curve calculated for diffraction scattering from a black disk of radius  $R = 1.32 \times A^{1/3}$  fermis (see Fig. 1). The total cross section obtained is about 1400 mb for the mixture C, O, N, and AgBr. This value is twice that for the reaction cross section. The Rutherford scattering curve from a point nucleus is also shown for comparison. The fact that the observed diffraction cross section lies above the Rutherford scattering curve for angles greater than 10 deg is



MU-14737

Fig. 1. K<sup>-</sup> nucleon elastic scattering differential cross section. The experimental cross section is compared with a point Rutherford scattering and diffraction scattering from a black disk of radius  $1.32 \times A^{1/3}$  fermis.

presumably due to interference phenomena including the real and imaginary part of both the Rutherford and diffraction-scattering amplitudes. This result is consistent with constructive interference between Coulomb and  $K^-$  nuclear scattering. A definite conclusion on this point must, however, await the completion of a detailed analysis.

### 3. The $K^-$ -H Cross Section

In the 33.0 meters scanned along the  $K^-$  track, we have found only one  $K^-$ -H scattering event and one  $K^-$ -H absorption event. To get a reasonable evaluation of the cross section, we have compiled published results,<sup>13, 14</sup> which are given in Table III. From these data one obtains a  $K^-$ -H scattering cross section of  $48.4^{+15}_{-11}$  mb, a  $K^-$  absorption cross section of  $11.4^{+9}_{-5}$  mb, and a total  $K^-$ -H cross section of  $60^{+15}_{-13}$  mb. The small number of  $K^-$ -H events found in this work must be attributed to a statistical fluctuation.

### III. $K^-$ -HYDROGEN ABSORPTION AT REST

In the course of this work, five events have been observed which we interpret as the absorption of stopped  $K^-$  mesons in hydrogen.<sup>15</sup> At the 1955 Pisa Conference<sup>1, 16</sup> we reported four of these events. At that time we were able to proceed only to the point of stating that if the  $K^-$  mesons involved possessed a unique mass value, then the  $\Sigma^-$  hyperon is heavier than the  $\Sigma^+$  hyperon by about  $14 m_e$ .

Recently, Budde et al. have confirmed our observation by an independent method in which the  $Q$  value of the  $\Sigma^-$  hyperon was measured directly.<sup>17</sup> Further confirmation was also found in emulsions in which the  $\Sigma^-$  decay in flight was observed<sup>18</sup> and the  $Q$  value was measured from the range of the decay pion. In addition, various authors have found other examples of  $K^-$ -H absorption in emulsion.<sup>14, 19, 20</sup> All these results confirm the observation that the  $\Sigma^- - \Sigma^+$  mass difference is about  $14 m_e$ .

We have reevaluated our data, based on new and more elaborate measurements, which now allow us to obtain the  $K^-$  mass in addition to the  $\Sigma^- - \Sigma^+$  mass difference. The five events that have been identified as the absorption of  $K^-$  mesons in hydrogen can be classified according to the following two reaction schemes:

Table III

Compilation of $K^-$ -hydrogen interaction events				
Group	Energy interval (Mev)	Number of absorptions in flight	Number of K-H scattering events	Path length (meters)
This work	16 to 150	1	1	33
White et al. <sup>a</sup>	16 to 150	1	10	30
Barkas et al. <sup>b</sup>	30 to 90	2	6	49.5
Combined	16 to 150	4	17	112.5

<sup>a</sup>See Ref. 13.  
<sup>b</sup>See Ref. 14.



In two events ( $K_{20}$  and  $K_{4003}$ ) of type (a), the  $\Sigma^+$  hyperons come to rest and decay by the processes  $\Sigma^+ \rightarrow \pi^+ + n$  and  $\Sigma^+ \rightarrow p + \pi^0$  respectively. The measured ranges of the hyperons are  $806.4 \pm 13\mu$  and  $804.9 \pm 13\mu$ , respectively. In two other events, ( $K_{MH-2}$  and  $K_2$ ), which we ascribe to Reaction (b), the  $\Sigma^-$  hyperons do not give capture stars at the ends of their ranges. Their respective ranges are  $694.1 \pm 22\mu$  and  $687 \pm 10\mu$ .

The errors quoted are all standard errors and include the observational errors, uncertainty in emulsion shrinkage, and Bohr straggling. The fifth event,  $K_{MH-1}$ , gives rise to a pion collinear with a  $\Sigma$  hyperon of  $574\mu$  range, which then decays into a  $\pi$  meson. The dip angle of the  $\Sigma$  hyperon is 45 deg, which is too steep to determine whether or not the  $\Sigma$  hyperon came to rest prior to its decay. The most plausible explanation



for this event is that it represents a K-H absorption event in which the positive or negative  $\Sigma$  hyperon decays in flight.

#### A. The $\Sigma^- - \Sigma^+$ Mass Difference

The mean  $\Sigma^+$  range for our events is  $806.0 \pm 11.5\mu$  and the mean  $\Sigma^-$  range is  $689.0 \pm 9.4\mu$ . If we assume a unique  $K^-$  mass equal to the  $K^+$  mass ( $966.17 m_e$ ), then Reactions (a) and (b) give  $M_{\Sigma^-} - M_{\Sigma^+} = Q_1 - Q_2$ . We take  $M_{\pi^+} = M_{\pi^-}$  according to Cohen, Crowe, and Dumont.<sup>21</sup> The new range-energy curve of Barkas et al.<sup>22</sup> was used to determine the  $\Sigma^- - \Sigma^+$  mass difference from the hyperon ranges. The result obtained in this way is insensitive to small variations in the stopping power of the emulsion and the value of the  $K^-$  mass. The data yield the value  $M_{\Sigma^-} - M_{\Sigma^+} = (13.9 \pm 1.8)m_e$ .

#### B. The $K^-$ Mass

The  $K^-$  mass can now be determined from the reactions that yield  $\Sigma^+$  hyperons, where the accuracy of the  $K^-$  mass is limited by the accuracy to which the  $\Sigma^+$  mass is known ( $M_{\Sigma^+} = (2327.4 \pm 1.0)m_e$ <sup>23</sup>) and the uncertainty in our  $\Sigma^+$  range determination. In this case, the uncertainty in emulsion density, resulting in an uncertainty in stopping power, does not cancel out. We determined the emulsion density from the ranges of protons from four  $\Sigma^+$  decays ( $\Sigma^+ \rightarrow p + \pi^0$ ) to an accuracy of  $\pm 1\%$ .

The proton ranges were:

$$1637.9 \pm 3.4\mu$$

$$1630.8 \pm 13.0\mu$$

$$1645.2 \pm 23.2\mu$$

$$1636.8 \pm 22.7\mu$$

This datum and the measured  $\Sigma^+$  ranges from Reaction (1) lead to a value for the  $K^-$  mass of  $966.7 \pm 2.0 m_e$ .

IV. THE  $K^-$  ABSORPTION STARS

As has been shown earlier,<sup>24, 16</sup> the  $K^-$ -meson absorption obeys the Gell-Mann selection rule for strong interactions, i. e.,  $\Delta S = 0$ . This selection rule requires the emission of a strange particle. To satisfy the strangeness selection rule and energy conservation, the absorption of negative  $K$  mesons at rest can lead only to emission of hyperons, i. e.  $\Lambda^0$  or  $\Sigma^{\pm, 0}$ .<sup>25</sup> Through the study of the interaction products of the absorption process at rest, we tried to determine the ratio of  $\Lambda^0$  to  $\Sigma^{\pm, 0}$  produced in the primary interaction. In Table IV we summarize the possible  $K^-$  reaction with one and two nucleons, respectively.<sup>26</sup>

Table IV

Interactions of $K^-$ mesons with one and two nucleons			
Interaction	Q (Mev)	Interaction	Q (Mev)
(1) $K^- + p \rightarrow \Sigma^+ + \pi^-$	103	(8) $K^- + p + p \rightarrow \Sigma^+ + n$	242
(2) $K^- + p \rightarrow \Sigma^- + \pi^+$	96	(9) $K^- + p + p \rightarrow \Sigma^0 + p$	244
(3) $K^- + p \rightarrow \Sigma^0 + \pi^0$	109	(10) $K^- + p + p \rightarrow \Lambda^0 + p$	317
(4) $K^- + p \rightarrow \Lambda^0 + \pi^0$	182	(11) $K^- + p + n \rightarrow \Sigma^0 + n$	244
(5) $K^- + n \rightarrow \Sigma^- + \pi^0$	102	(12) $K^- + p + n \rightarrow \Lambda^0 + n$	317
(6) $K^- + n \rightarrow \Sigma^0 + \pi^-$	105	(13) $K^- + p + n \rightarrow \Sigma^- + p$	237
(7) $K^- + n \rightarrow \Lambda^0 + \pi^-$	179	(14) $K^- + n + n \rightarrow \Sigma^- + n$	237

We have estimated the interactions with two nucleons from the energy spectrum of the hyperons to be no more than 10% of all interactions. In this analysis, we have treated the case of  $K^-$  interactions with only a single nucleon, which should thus comprise more than 90% of all interactions.

A. The Pion Spectrum

In nuclear emulsions one cannot, in general, detect the neutral hyperons correlated with a given  $K^-$ -absorption star. Therefore, to arrive at the ratio of  $\Lambda^0$  to  $\Sigma^{\pm,0}$  hyperons at production, one has to utilize indirect information. Such information can be obtained from the charged pions produced in association with  $\Sigma$  and  $\Lambda$  hyperons. Assuming charge independence, we can express the  $\Lambda^0$  to  $\Sigma^{\pm,0}$  production ratio in terms of the charged pions produced in association with the hyperons. Table V summarizes for all  $K^-$  reactions with one nucleon the probabilities of hyperon production, for the mixture of isotopic-spin singlet and triplet states. The production amplitudes for the reactions giving  $\Sigma$  and  $\Lambda$  hyperons are designated by A and B, respectively. Subscripts 0 and 1 refer to  $T = 0$  and  $T = 1$ ;  $\phi$  is the interference angle between the two states.

Table V

Hyperon production from $K^-$ -nucleon reactions	
Reaction	Transition probability
$K^- + p \rightarrow \pi^0 + \Lambda^0$	$1/2 B_1^2$
$K^- + p \rightarrow \pi^+ + \Sigma^-$	$1/6 A_0^2 + 1/4 A_1^2 + 1/\sqrt{6} A_0 A_1 \cos \phi$
$K^- + p \rightarrow \pi^0 + \Sigma^0$	$1/6 A_0^2$
$K^- + p \rightarrow \pi^- + \Sigma^+$	$1/6 A_0^2 + 1/4 A_1^2 - 1/\sqrt{6} A_0 A_1 \cos \phi$
$K^- + n \rightarrow \pi^- + \Lambda^0$	$B_1^2$
$K^- + n \rightarrow \pi^0 + \Sigma^-$	$1/2 A_1^2$
$K^- + n \rightarrow \pi^- + \Sigma^0$	$1/2 A_1^2$

Let us designate pions produced in association with  $\Sigma$  and  $\Lambda$  hyperons as  $\pi_{\Sigma}$  and  $\pi_{\Lambda}$ , respectively. Then from the above equations it can easily be seen that for a neutron-to-proton ratio of unity ( $n/p = 1$ ), we have

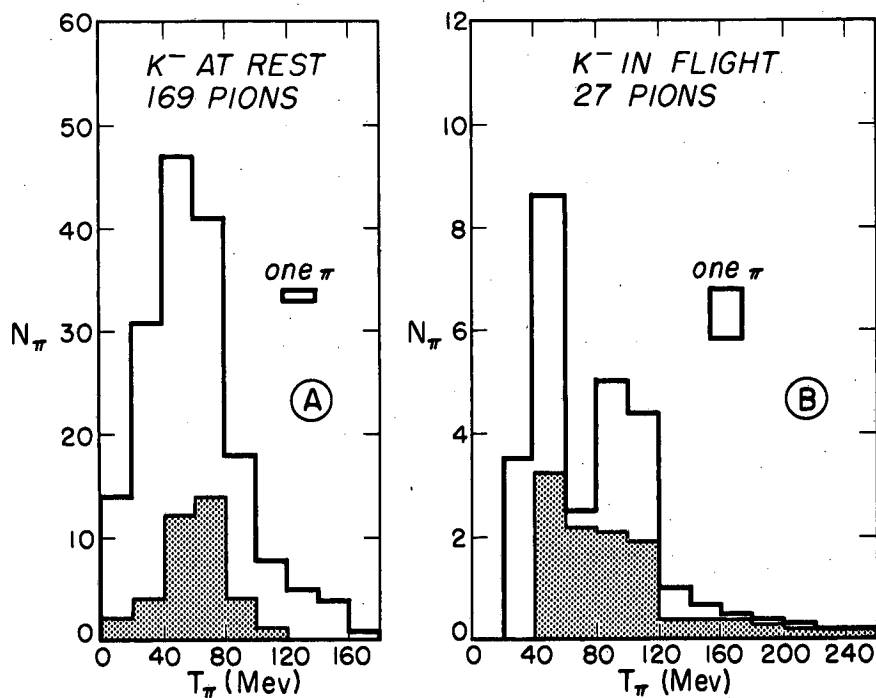
$$\pi_{\Lambda}^{-} / (\pi_{\Sigma^{+},0}^{-} + \pi_{\Sigma^{-}}^{+}) = \Lambda^{0} / \Sigma^{\pm,0} = B_1^2 / 1/3(A_0^2 + A_1^2).$$

Taking into account that the  $n/p$  ratio averaged over emulsion nuclei is  $n/p = 1.2$ , we obtain

$$0.93 \left[ \pi_{\Lambda}^{-} / (\pi_{\Sigma^{+},0}^{-} + \pi_{\Sigma^{-}}^{+}) \right] \simeq \Lambda^{0} / \Sigma^{\pm,0}.$$

The charged-pion ratio can be obtained from the pion spectrum. An inspection of Table IV tells us that the  $Q$  values for the reactions producing  $\Lambda$  hyperons is larger by  $\sim 80$  Mev than that for producing  $\Sigma$  hyperons. Therefore the respective pion energies would differ by about 60 Mev. The analysis of the pion spectrum would thus yield direct information on the  $\Lambda/\Sigma$  ratio at production.

Figure 2 shows a comparison of the pion spectrum from absorption stars in flight and at rest. Part of this pion spectrum at rest was presented by one of us at the sixth Annual Rochester Conference.<sup>1</sup> To the spectrum consisting of 124 pions presented at that time, we have added 45 new measurements selected as an unbiased sample from 226 additional  $K^{-}$  interactions at rest. The selection consisted of all pions of dip angle less than 20 deg. The shaded region in Fig. 2 indicates the pions associated with identified  $\Sigma$  hyperons. Considering the absorption stars at rest only, we can see that qualitatively there is no appreciable difference (except for a small high-energy tail) between the entire pion spectrum and those pions produced in association with identified  $\Sigma$  hyperons. This indicates that the  $\Sigma$  production is the dominant interaction process in  $K^{-}$ -absorption events, as was pointed out earlier.<sup>1</sup> This result has been observed by Alvarez et al.<sup>6</sup> to occur also in the absorption of  $K^{-}$  mesons in pure hydrogen. In the next section we discuss a quantitative evaluation of the  $\Lambda/\Sigma$  ratio.



MU-14738

Fig. 2. The charged-pion spectrum.  
 A. A histogram of the observed pion spectrum from K<sup>-</sup> interactions at rest.  
 B. An ideogram of the observed pion spectrum from K<sup>-</sup> interactions in flight.  
 The shaded region represents the pions produced in association with identified charged hyperons.

### 1. The $\Lambda/\Sigma$ Ratio

In order to analyze the pion spectrum in terms of  $\pi_{\Sigma}$  pions and  $\pi_{\Lambda}$  pions, we first computed the pion spectrum that would result from Reactions (1), (2), and (6) alone and from Reaction (7) alone (see Table IV). The pion spectrum has been computed by use of the Serber model. The calculations leading to the comparison with the observed spectra have been arrived at by the following steps:<sup>27</sup>

(a) A  $K^{-}$  meson bound in the atomic orbit around a nucleus interacts with a single nucleon whose momentum is given by a Gaussian momentum distribution. The  $1/e$  value has been taken to be 20 Mev.

(b) The resulting pion and hyperon are produced inside the nucleus in accordance with conservation of energy and momentum in the center-of-mass system, taking into account the potentials in which these particles find themselves. The values we have assumed are:

$$V_{\Sigma} = V_{\Lambda} = -15 \text{ Mev,}$$

$$V_{K} = 0 ,$$

$$V_{\pi} = -40 \text{ Mev,}$$

$$V_{N} = -42 \text{ Mev.}$$

(c) In order to obtain the pion and hyperon spectrum outside the nucleus, we altered their energies by adding their respective well depths.

(d) An additional modification of the pion spectrum is due to the energy dependence of the mean free path of pions in nuclear matter. This has the effect of reducing the high-energy part of the spectrum while enhancing the spectrum around 35 Mev (inelastic scattering). The calculations have been carried out for two extreme models: (1) uniform absorption of the  $K^{-}$  meson, and (2) surface absorption of the  $K^{-}$  meson (see appendix I for details).

In Table VI we give the resulting  $\Lambda/\Sigma$  ratios obtained by fitting the experimental pion spectrum with a superposition of the computed  $\pi_{\Lambda}$  and  $\pi_{\Sigma}$  spectra. The  $\Lambda/\Sigma$  ratio is given for the two extreme models and also for an intermediate model corresponding to the average between the two. The errors quoted are the statistical errors only. As can be seen, the ratio is quite sensitive to the radius  $R_a$  at which the absorption occurs.

Table VI

Fraction of $\pi_{\Lambda}^{-}/\pi_{\Sigma}^{\pm}$			
Type of model	At emission	At production	$\Lambda^0/\Sigma^{\pm,0}$
Surface	$0.20 \pm 0.04$	$0.23 \pm 0.05$	$0.21 \pm 0.07$
Homogeneous	$0.39 \pm 0.10$	$0.53 \pm 0.14$	$0.50 \pm 0.16$
Average	$0.25 \pm 0.06$	$0.31 \pm 0.08$	$0.28 \pm 0.10$

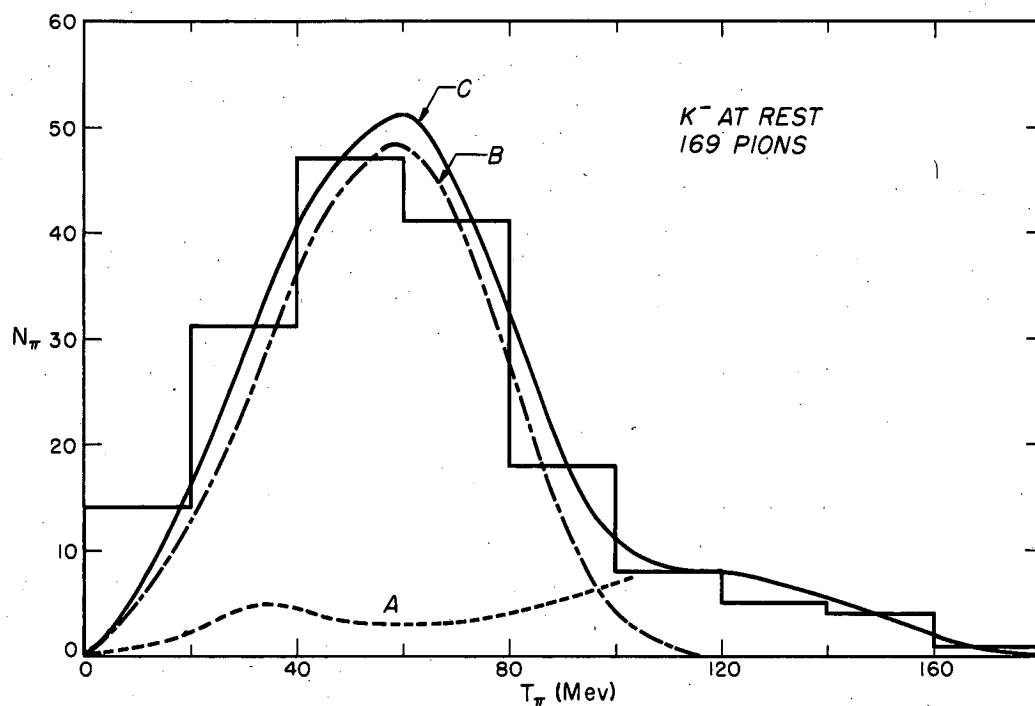
Figure 3 shows the experimental pion spectrum together with the fit obtained from the theoretical spectrum computed for the intermediate case.

#### B. Comparison Between Absorption at Rest and in Flight

In the absorption at rest, the  $K^{-}$  meson is captured in  $K$ -mesonic Bohr orbits and is finally absorbed into the nucleus. If we define a radius  $R_a$  as the average distance from the center of the nucleus at which the absorption takes place, then this radius depends on (a) the  $K^{-}$  nucleon absorption cross section at the relative energy determined by the  $K$ -mesonic orbital energy and the Fermi energy of the nucleon, and (b) the overlap of the nuclear density distribution and the wave function for the orbit from which the absorption takes place.

The capture mechanism for  $K^{-}$  in flight consists of an absorption in a single traversal through the nucleus at impact parameter  $b$ . In this case,  $R_a$  is equal to the average impact parameter  $b$  at which the absorption occurs. Thus, the absorption radius  $R_a$  depends on the  $K^{-}$ -nucleon cross section at higher energies ( $T_{K^{-}} \approx 105$  Mev) and the nuclear density distribution.

The pion spectrum of interactions in flight is shown in Fig. 2B. Although the number of pions observed is small, the following observation can be made:



MU-14739

Fig. 3. Histogram of the charged-pion spectrum.  
A. The calculated spectrum of pions produced in association with  $\Lambda$  hyperons. Intermediate model.  
B. The calculated spectrum of pions produced in association with  $\Sigma$  hyperons. Intermediate model.  
C. Curves A and B combined.



(a) The shape of the total pion spectrum corresponds to the pattern of the pions associated with  $\Sigma$  hyperons in the same way as it does for interactions of  $K^-$  mesons at rest.

(b) The peak in the  $\pi_\Sigma$  spectrum expected at around 160 Mev (i. e.  $T_K = 105$  Mev in addition to the peak energy of 60 Mev observed for pions from  $K^-$  stars at rest) is shifted towards a lower energy and smeared over a large energy interval. The average expected kinetic energy of the pions under discussion here is about the same as that of pions associated with  $\Lambda$  hyperons at rest ( $\sim 150$  Mev). By comparing the observed pion spectrum with the calculated  $\pi_\Lambda$  spectrum for  $K^-$  absorption at rest, we see that the homogeneous model fits the spectrum better than the surface or average model.

We can use these data to obtain an estimate of the comparative absorption radius for  $K^-$  interactions in flight and at rest. If we consider the bubble chamber data of Alvarez et al.<sup>6</sup> and make use of charge independence, we expect the  $\Lambda/\Sigma$  ratio to be of the order of 0.2. This indicates that the data for the  $K^-$  interactions at rest are fitted best by a radius not much smaller than indicated by the surface model. We thus conclude that  $R_a$  at rest is greater than  $R_a$  in flight. This effect is similar to the one found for antiproton annihilation stars at rest and in flight.<sup>28</sup>

### C. $K^-$ Absorption Stars as a Source of $\Lambda^0$ -Hyperons

In the preceding section we have obtained from the observed pion spectrum the ratio of  $\Lambda^0$  to  $\Sigma^{\pm,0}$  hyperons produced. In this section we estimate the fraction of hyperons emitted in the average star formed by  $K^-$  interactions with nuclei in nuclear emulsion.

We have obtained this estimate by two methods:

1. energy balance;
  2. strangeness balance.
1. Energy Balance

From the observed energy in charged particles emitted in  $K^-$  interactions, we have evaluated the energy emitted in neutral particles.

In order to evaluate the average energy per star given to nucleons, we have phenomenologically divided the nucleons into two classes:

(a) Those due to the "knock-on" process in which,  $T_{\text{nucleon}}$  is 30 Mev or more, and (b) those due to the evaporation process in which,  $T_{\text{nucleon}}$  is less than 30 Mev. The energy emitted in knock-on neutrons was obtained by using the average knock-on proton energy and a neutron-to-proton ratio  $\langle n/p \rangle = \langle (A-Z)/Z \rangle_{\text{emulsion}} = 1.2$ . The energy emitted in evaporation neutrons was obtained from the observed frequency of evaporation protons<sup>29</sup> and by using an  $n/p$  ratio of 4 with an average neutron kinetic energy of 3 Mev.<sup>30</sup>

The average energy per star given off in pions and hyperons has been obtained from the observed pion and hyperon spectra. A correction factor had to be applied to this average energy to take into account the detection efficiency for these particles. We estimate the detection efficiency for the charged pions as 90 %, for  $\Sigma^+$  hyperons about 95%, and for  $\Sigma^-$  hyperons about 50 %. The low detection efficiency for  $\Sigma^-$  hyperons is due to the frequent formation of zero-prong stars in  $\Sigma^-$  absorption.

To estimate the energy in neutral pions and  $\Sigma^0$  hyperons, we have used charge independence and have assumed the same amount of attenuation for the neutral particles as for their charged counterparts on leaving the nuclei in which they were formed. Table VII summarizes the numerical values obtained. We can now determine the average energy  $\bar{E}_0$  in neutral particles other than in neutrons, neutral pions, and  $\Sigma^0$  hyperons. We have

$$\begin{aligned} \bar{E}_0 &= M_K - (B_K + B_N) - \bar{U} \\ &= 495 - (8 + 8) - 331 \text{ Mev} \\ &= 146 \text{ Mev,} \end{aligned}$$

where  $B_K$  and  $B_N$  are the atomic binding energies of the K meson and the binding energy of the last nucleon in the nucleus, respectively. The 146 Mev carried away by other neutral particles we attribute to  $\Lambda$  hyperons. The  $\Lambda$  hyperons arise from two sources: (a) the primary process,  $K^- + "n" \rightarrow \Lambda^0 + \pi^-$ , and (b) the secondary process, interactions of  $\Sigma$  hyperons with nucleons in the same nucleus in which they are produced, i. e.

Table VII

Division of energy released in an average  $K^-$  star

<u>Particles</u>		<u>Energy (Mev)</u>	<u>Source of data</u>
Evaporation nucleons	$\bar{U}_{ex}$	77	This work
Knock-on nucleons	$\bar{U}_{ko}$	62	This work
Charged pions	$\bar{U}_{\pi^\pm}$	67	1956 Rochester compilation <sup>1</sup>
Charged hyperons	$\bar{U}_{\Sigma^\pm}$	58	1956 Rochester compilation <sup>1</sup>
Hyperfragments	$\bar{U}_{hyperon}$	5	This work
Neutral pions	$\bar{U}_{\pi^0}$	33	inference from charge independence
Neutral hyperons	$\bar{U}_{\Sigma^0}$	29	inference from charge independence
Energy accounted for	$\bar{U}$	331	

$\Sigma + "n" \rightarrow \Lambda^0 + "n"$ . In both these processes the  $\Lambda^0$  hyperons are emitted with an average kinetic energy of  $T_\Lambda \approx 40$  Mev. The fraction of  $K^-$  stars in which a  $\Lambda^0$  particle is emitted as a final product is then given by

$$f_{\Lambda^0} = \frac{\overline{E}_0}{M_\Lambda - M_p + T_\Lambda} = \frac{146}{217} = 0.67,$$

where  $M_\Lambda$  and  $M_p$  are the  $\Lambda^0$  mass and proton mass respectively, in Mev.

## 2. Strangeness Balance

Conservation of strangeness requires that in each  $K^-$  interaction either a  $\Sigma$  or  $\Lambda$  hyperon be emitted. From the observed number of  $\Sigma$  hyperons and hyperfragments emitted, we can estimate the amount of missing strange particles. In this evaluation we have taken into account the low detection efficiency for  $\Sigma^-$  ( $\sim 50\%$ ), and have used charge independence to estimate the amount of  $\Sigma^0$ -hyperon production. Table VIII summarizes the observed and inferred percentages of emitted  $\Sigma$  hyperons. From Table VIII it can be seen that we can account for strange particles in 35% of the stars. From this figure we deduce that in the remaining 65% of the stars,  $\Lambda$  hyperons must have been emitted. Combining these two results we obtain  $f_\Lambda = 0.66$ . The fraction of  $\Lambda$  hyperons emitted in  $K^-$  stars and the  $\Lambda/\Sigma$  ratio at production (Section IIIA) permit an evaluation of the amount of  $\Sigma$ -to- $\Lambda$  conversion on leaving the parent nucleus. We find 58% of the  $\Sigma$  hyperons are converted into  $\Lambda$  hyperons.

We have thus shown by two independent methods that  $K^-$  interactions with bound nucleons in complex nuclei give as their final product mainly  $\Lambda$  hyperons. This effect may thus be utilized as a source for  $\Lambda$  hyperons for the detailed investigation of their properties.

## 3. Prong Distribution and Visible Energy Release

The average kinetic energy for the stars in flight is  $\overline{T}_K = 105$  Mev. This additional kinetic energy expresses itself in a larger nuclear excitation, as can be observed by comparing Figs. 4 and 5, parts a and b, which give the prong distribution and visible-energy release for the interactions at rest and in flight respectively.

Table VIII

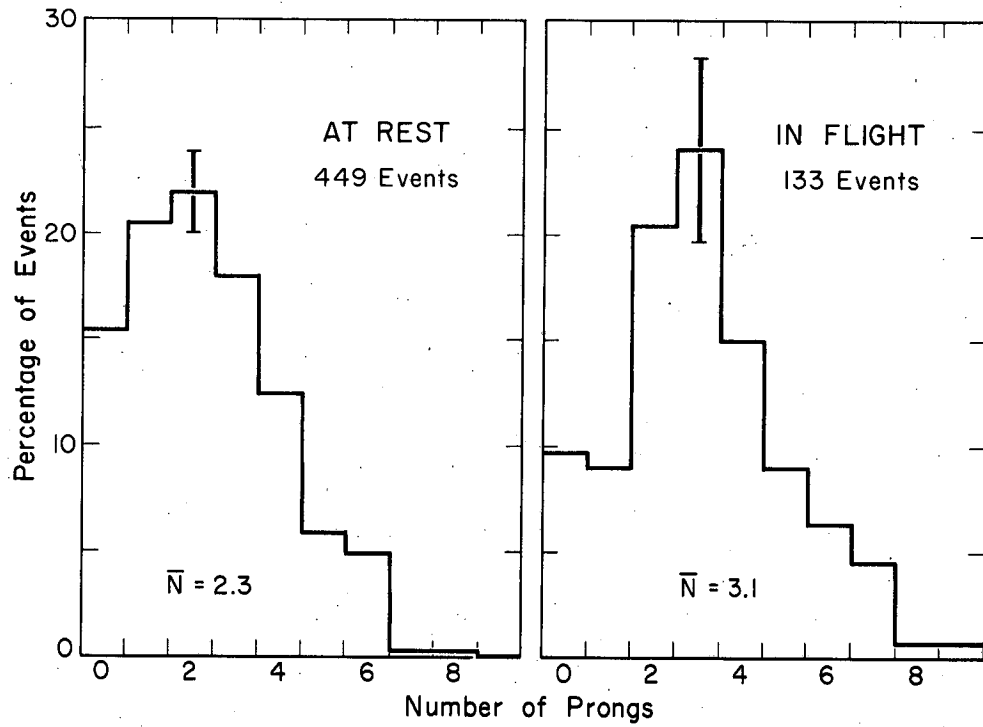
Strangeness balance		
Type	Percent hyperon emission	Source
$\Sigma^{\pm}$	14	Observed
$\Sigma^{-}$	7	Detection efficiency correction
$\Sigma^0$	10	Charge independence
H <sub>F</sub>	3	Observed
Trapped $\Lambda^0$	1	Observed
	35%	

### V. OBSERVATIONS ON $\Sigma$ HYPERONS

In the course of this work we have identified 19  $\Sigma^+$ , 6  $\Sigma^{\pm}$ , and 16  $\Sigma^-$  hyperons from  $K^-$  stars at rest and 5  $\Sigma^+$ , 6  $\Sigma^{\pm}$ , and 2  $\Sigma^-$  hyperons from  $K^-$  stars in flight. In Table IX we list the pertinent information on the  $\Sigma^+$  and  $\Sigma^{\pm}$  hyperons, and in Table X the information on  $\Sigma^-$  hyperons.

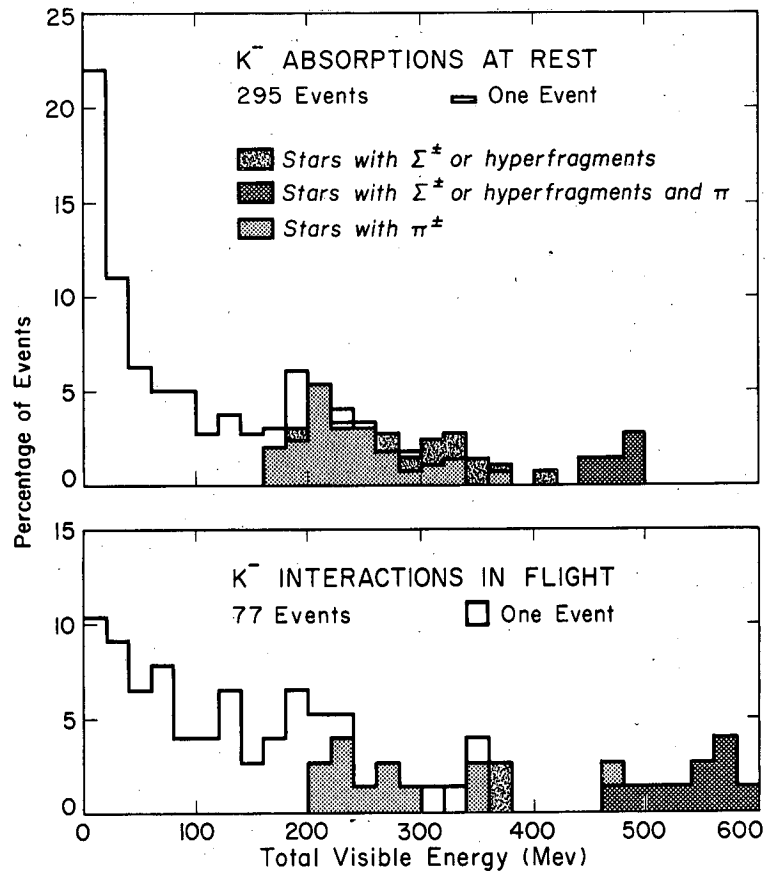
In this work we do not have a sufficiently large sample to attempt a statistical analysis of the properties of the  $\Sigma$  hyperons, viz., lifetimes,  $\Sigma^+$  mass, and decay asymmetries or asymmetries in the triple scalar product, such as  $P_{\Sigma} \times P_{\pi} \cdot P_{\pi\Sigma}$ , etc. We will thus present our data here only to make them available for inclusion in future compilations.

It is noteworthy that event S<sub>20</sub> gives a  $\Sigma^+$  hyperon that we have classified as a  $\Sigma^+ \rightarrow p + \pi^0$  decay at rest for which the decay proton has an exceptionally long range,  $R_p = 1864 \mu$ . This can have a number of explanations:



MU-14740

Fig. 4. Histogram of prong distribution of  $K^-$  absorption events.  
A. Absorption at rest.  
B. Absorption in flight.



MU-14741

Fig. 5. Histogram of total visible energy release in K<sup>-</sup> absorption events.  
A. Absorption at rest.  
B. Absorption in flight.

Table IX

Characteristics of $\Sigma^+$ and $\Sigma^0$ hyperons from K <sup>+</sup> stars								
Event	Range of $\Sigma$ ( $\mu$ )	Kinetic energy of $\Sigma$ at K <sup>+</sup> star	Range of proton if in p + $\pi^0$ mode	Cosine of space angle of decaying pion	Associated $\pi$ meson (if present)	Kinetic energy of $\pi$ meson <sup>b</sup> (Mev)	Time to point of decay ( $\times 10^{-10}$ sec)	Potential time ( $\times 10^{-10}$ sec)
<u>Decay of <math>\Sigma^+</math> to n + <math>\pi^+</math> at rest</u>								
K114	11240	64	—	+0.492	—	—	—	1.79
K20 <sup>a</sup>	806.4	13.7	—	+0.158	$\pi^-$	100	—	0.232
S11B	3303	31.2	—	-0.422	$\pi^+$	—	—	0.712
S23	4375	36.8	—	-0.175	$\pi^-$	178	—	0.867
S1003	1944	22.8	—	+0.911	—	—	—	0.485
K1	620	11.7	—	+0.517	—	—	—	0.206
K5	363	8.6	—	-0.919	—	—	—	0.144
K14	950	15.1	—	+0.013	$\pi^+$	98	—	0.280
K18	1510	20.0	—	+0.956	$\pi^+$	48	—	0.396
K21 <sup>a</sup>	1385	19.6	—	-0.059	$\pi^+$	55	—	0.369
K28	475	10.1	—	+0.895	$\pi^+$	125	—	0.173
K33	930	14.8	—	-0.231	$\pi^-$	49	—	0.270
K44	1320	18.3	—	+0.812	—	—	—	0.350
K50	1805	21.9	—	-0.187	—	—	—	0.445
K1023	2300	25.3	—	-0.226	$\pi^-$	27	—	0.538
<u>Decay of <math>\Sigma^+</math> to p + <math>\pi^0</math> at rest</u>								
K <sup>77</sup>	105	4.1	1631	+0.478	—	—	—	0.96
K <sup>73</sup>	2840	28.5	1638	-0.470	—	—	—	0.63
KC31	960	15.5	1645	-0.558	—	—	—	0.39
K1036	716	12.7	1580	+0.352	$\pi^+$	67	—	0.23
K4003 <sup>a</sup>	804.9	13.7	1637	-0.869	$\pi^+$	77	—	0.22
K10	356	8.5	1600	+0.943	—	—	—	0.14
K52	1436	19.3	1596	-0.051	$\pi^+$	71	—	0.38
S9	6850	47.8	1669	+0.661	$\pi^+$	100	—	1.25
S20	5590	42.3	1864	-0.690	$\pi^+$	89	—	1.03
<u>Decay of <math>\Sigma^+</math> to p + <math>\pi^0</math> in flight</u>								
KL11	2560	35.0	2920	-0.788	—	—	0.23	0.80
K1049	1780	52.0	16,100	+0.945	$\pi^+$	58	0.86	1.30
K1002	19800	122	22,400	-0.890	—	—	2.17	3.77
K1008	1250	31.4	18,900	-0.930	$\pi$ (?)	—	0.36	0.70
<u>Decay of <math>\Sigma^0</math> to n + <math>\pi^0</math> in flight</u>								
K6011	19	13	—	-0.693	$\pi^+$	—	0.007	0.242
K1038	13000	95	—	+0.160	—	—	1.25	2.75
S4	6040	59	—	+0.253	$\pi^+$	—	0.72	1.52
S8	4880	80	—	-0.147	$\pi^+$	—	0.42	2.20
S138	23000	137	—	+0.313	$\pi^+$	—	1.71	4.31
S24	836	120	—	+0.432	—	—	0.03	3.65
S1006	2010	46	—	-0.930	$\pi^+$	—	0.26	1.11
S1024	2035	64	—	+0.769	$\pi^+$	—	0.20	1.07

<sup>a</sup>K-H absorption events  
<sup>b</sup>Given only for events in which dip angle was not greater than 20 deg.



Table X

Characteristics of  $\Sigma^-$  hyperons from  $K^-$  stars

Event	Range of $\Sigma^-$ (microns)	Kinetic energy (Mev)	No. of prongs of $\Sigma^-$ star	Range of prongs <sup>a</sup> (microns) and comments	Identified	Associated $\pi$ meson (if present)	Kinetic energy of associated $\pi$ meson (Mev)
$K^-_2$	695	12.6	0	$\Sigma p$ from $K^- + H$ absorption. from kinematics		$\pi^\pm$	85
$K^-_{C2}$	815	13.8	2	168, 87			—
$K^-_6$	254	7.0	1	< 30		$\pi^\pm$	55
$K^-_9$	4100	35.0	1	< 30			—
$K^-_{C10}$	76	33.0	1	955 and 1 recoil		$\pi^+$	57
$K^-_{M13}$	547	11.0	2	6080, 5760 and 1 recoil			—
$K^-_{14}$	3433	32.0	0	$\Sigma p$ with associated electron			—
$K^-_{16}$	1970	23	1	< 30			—
$K^-_{19}$	181	5.1	0	$\Sigma p$ with associated electron			—
$K^-_{C22}$	3100	30.0	5	205, 1800, 50, 204, 390 and 1 recoil			—
$K^-_{63}$	222	6.4	1	1195; d or $\alpha$ particle		$\pi^\pm$	83
$K^-_{1001}$	974	15.4	1	594		$\pi^-$	24
$K^-_{1004}$	827	14.0	1	1730 and 3 recoils			—
$K^-_{1060}$	1068	16.2	1	37			—
$K^-_{4001}$	632	12.2	1	293 and 2 recoils		$\pi^\pm$	84
$K^-_{5018}$	184	5.7	2	546, 176		$\pi^\pm$	77
$S^-_3$	2550	27.3	1	695		$\pi^+$	54
$S^-_{148}$	1919	23.1	1	4250			—

<sup>a</sup>all prongs are consistent with protons unless stated otherwise.

(a) the  $\Sigma^+$  was not quite at rest;

(b) this is a prong from a  $\Sigma^-$  star;

(c) it must be borne in mind that long-lived excited states of  $\Sigma$  hyperons might exist, which could then decay with a higher  $Q$  value. It is thus important to observe the range distribution and watch for possible fine structure. A similar case was reported by Fry et al.<sup>31</sup> with  $R_p = 1800\mu$ .

Using the eight  $\Sigma^\pm$  hyperons decaying in flight (Table IX) we obtain, from a maximum-likelihood analysis,  $\tau_{\Sigma^\pm} = 0.813^{+1.25}_{-0.34} \times 10^{-10}$  sec.<sup>32</sup> This value is quite consistent with the  $\Sigma^+$  and  $\Sigma^-$  lifetime and does not give the anomalously low values obtained by Fry et al.<sup>33</sup> and Glasser et al.<sup>34</sup>

### ACKNOWLEDGMENT

We wish to thank Dr. Edward J. Lofgren and the Bevatron crew for their excellent support and cooperation. We are especially grateful to Mr. Hugo Bayona, Mrs. Frances Glenn, Miss Graydon Hindley, Mr. D.H. Kouns, Miss Sheila Livingston, Miss Helen Probst, Mrs. Evelyn Rorem, Mrs. Elisabeth Russel, Mrs. Louise Shaw, Mrs. Catherine Toche and Mr. G.M. Wike for their constant assistance throughout this work. We particularly appreciate the assistance of Miss Susan Klein in the compilation of the data. We are indebted to Dr. Robert Karplus for the many helpful discussions.

This work was done under the auspices of the U.S. Atomic Energy Commission.

## APPENDIX

To evaluate the effect of pion absorption on leaving the nucleus, we have used an optical model. We have applied the pion mean free path as given by Frank, Gammel, and Watson (FGW)<sup>35</sup> to two extreme cases. In the first case, we assume that the  $K^-$  mesons are absorbed uniformly over the volume of the nucleus (homogeneous model). The fraction of pions leaving the nucleus without interacting is then given by the formula

$$f_T = 3 \left[ \frac{1}{2x} - \frac{1}{x^3} (1+x) e^{-x} \right],$$

where  $x = \frac{2R}{\lambda}$ ;  $\lambda$  = mean free path in nuclear matter; and  $R = 1.4 \times A^{1/3} \times 10^{-13}$  cm is the nuclear radius.<sup>36</sup> (The parameter  $r_0 = 1.4 \times 10^{-13}$  cm must be used in this calculation, because the mean free path was computed for this value by FGW).

In the second case we consider the other extreme, in which we assume that all  $K^-$  mesons are absorbed on the surface of the nucleus, i. e.; a shell of radius  $R$  (surface model). The fraction of pions leaving the nucleus is now given by  $f_T = \frac{1}{2} \left[ 1 + (1 - e^{-x})/x \right]$ . Figure 6 gives the percentage of pions emitted from the nucleus without interactions, averaged over the emulsion constituents for the two cases. For the mean free path  $\lambda$ , we have used  $\lambda_T$ , the total mean free path. We thus have  $1/\lambda_T = 1/\lambda_a + 1/\lambda_s$ , where  $\lambda_a$  = absorption mean free path and  $\lambda_s$  = scattering mean free path.

The fraction of pions emitted,  $f_T$ , corresponds thus to those pions that do not undergo any nuclear interaction. The fraction  $1 - f_T$  corresponds to those pions that are absorbed or elastically scattered from a nucleon inside the complex nucleus. Those pions that are scattered inside the nucleus can undergo subsequent collisions and are either absorbed or finally emitted at a lower energy. Thus the final pion spectrum consists of the unmodified pions that are a fraction  $f_T$  of the pions produced in the  $K^-$ -nucleon absorption process, and superimposed on this is the spectrum of the inelastically scattered pions (pions degraded in energy). To estimate the spectrum of the inelastically scattered pions, we have used the results

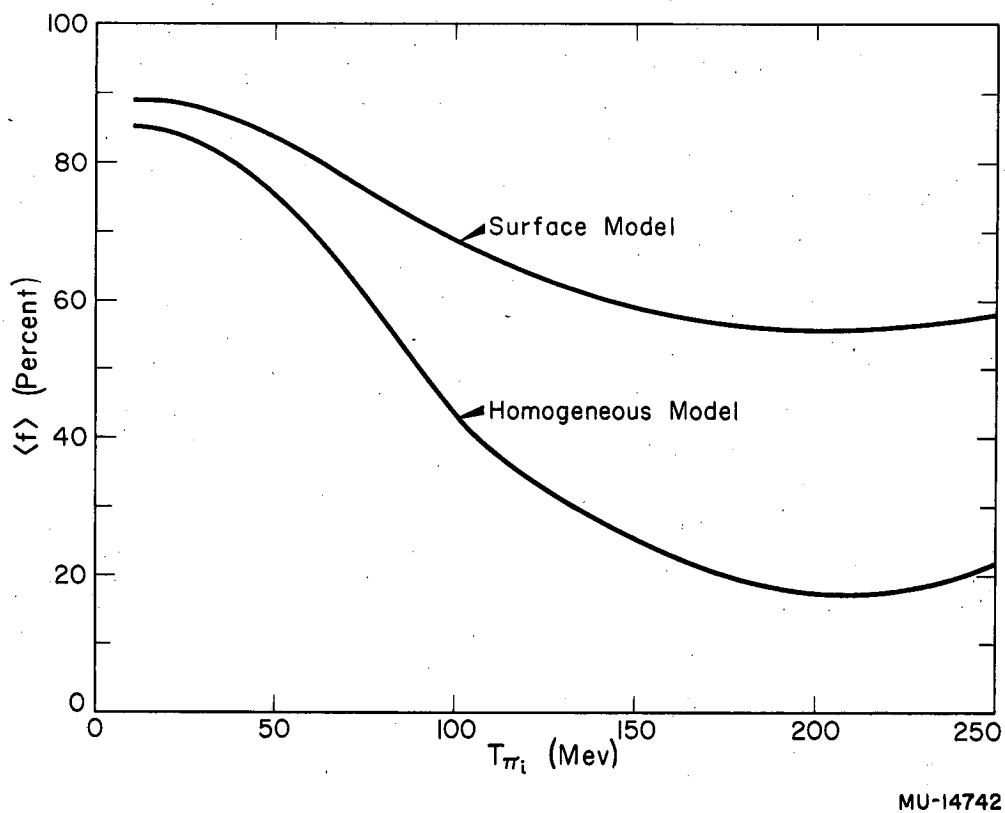
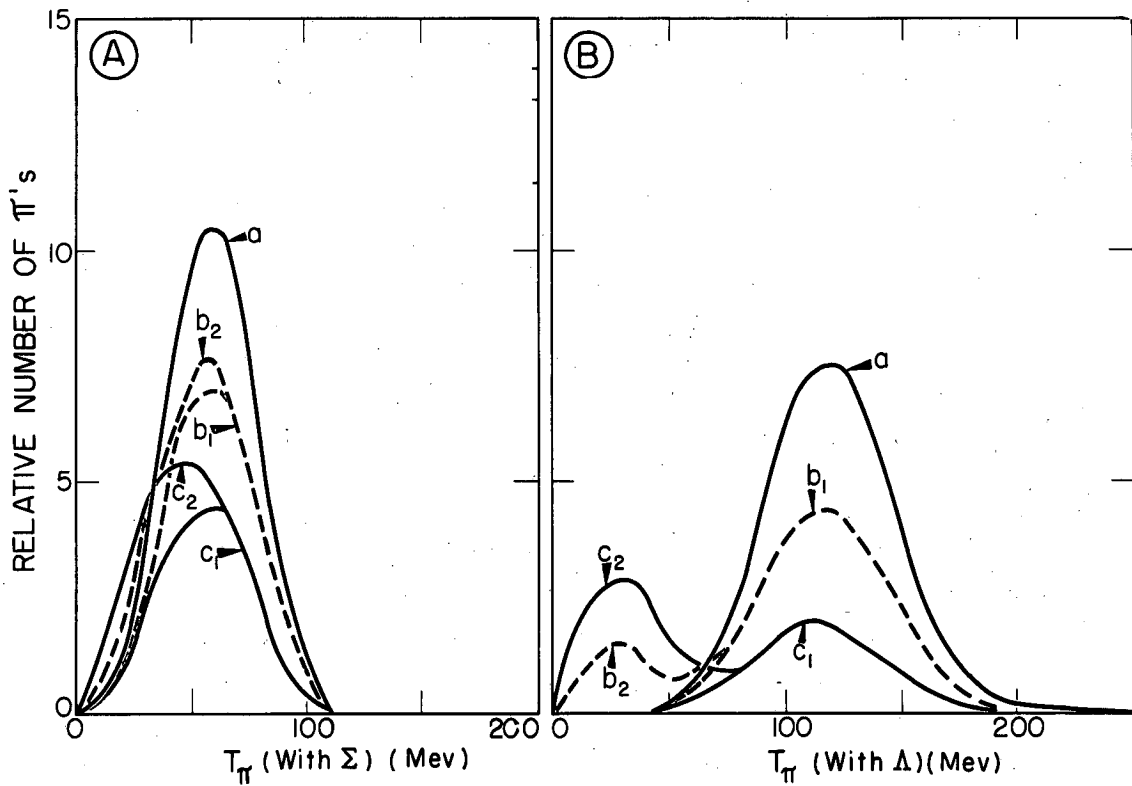


Fig. 6. Calculated elastic pion emission for the energy interval 0 to 250 Mev inside the nucleus. The upper curve is calculated for the surface model, and the lower curve for the homogeneous model, averaged over the constituents of photographic emulsions.

obtained in studies of pion interactions in nuclear emulsions in the energy range 60 to 150 Mev. In these experiments, it was shown that the inelastic scattering cross section is about 25% of the pion-reaction cross section and that the pions are degraded to a final energy centered at about 35 Mev.<sup>1, 37</sup> The fraction of inelastically scattered pions has thus been taken as  $0.25 (1 - f_T)$ .

In Fig. 6 we showed the percent pion emission  $f_T$  as a function of pion kinetic energy inside the nucleus for the two models under discussion. The effect of scattering and absorption for the pions produced in association with  $\Sigma$  and  $\Lambda$  hyperons is shown in Figs. 7A and 7B respectively, for both the surface and the homogeneous models. For comparison, the original production spectra are also shown. This calculation has been made for equal probabilities of production of  $\Sigma$  and  $\Lambda$  hyperons.



MU-14743

Fig. 7. The theoretical pion spectra associated with  $\Sigma$  and  $\Lambda$  production.

Curves a give the original pion distribution at production normalized in each case to the same total intensity.

Curves b and c show modifications due to pion absorption according to the surface and uniform models, respectively.

Subscripts 1 and 2 refer to the unmodified and total pion spectrum respectively.

REFERENCES

1. S. Goldhaber, in Proceedings of Sixth Annual Rochester Conference on High-Energy Physics; 1956 (Interscience, New York, 1956), Section VI, 1.
2. Iloff, Goldhaber, Goldhaber, Lannutti, Gilbert, Violet, White, Fournet, Pevsner, and Ritson, Phys. Rev. 102, 927 (1955).
3. Cork, Lambertson, Piccioni, and Wenzel, Phys. Rev. 106, 167 (1957).
4. Iloff, Chupp, Goldhaber, Goldhaber, and Lannutti, Phys. Rev. 99, 1617 (1955); V. Fitch and R. Motley, Phys. Rev. 101, 496 (1956), Alvarez, Crawford, Good and Stevenson, Phys. Rev. 101, 503 (1956).
5. Two of these have been published in an earlier communication: G. Ekspong and G. Goldhaber, Phys. Rev. 102, 1187 (1956).
6. Aggson, Fretter, Friesen, Hansen, Kepler, and Lagarrigue, Phys. Rev. 102, 243 (1956); and Alvarez, Bradner, Falk-Vairant, Gow, Rosenfeld, Solmitz, and Tripp, Nuovo cimento 5, 1026 (1957).
7. Birge, Perkins, Peterson, Stork, and Whitehead, Nuovo cimento 4, 834 (1956).
8. One additional K-H scattering event was found in another stack in which 2.4 meters of track length was scanned.
9. Very similar results were recently observed by the group at Göttingen, who have also drawn the same conclusions independently (M. Ceccarelli, private communication).
10. See, for example, Costa and Patergnani, Nuovo cimento 5, 448 (1957).
11. Igo, Ravenhall, Tieman, Chupp, Goldhaber, Goldhaber, Lannutti, and Thaler, Phys. Rev. (to be published).
12. George Igo (Stanford University), private communication.
13. Gilbert, Violet, and White, Bull. Am. Phys. Soc. II, 222 (1957).
14. Barkas, Dudziak, Giles, Heckman, Inman, Mason, Nickols, and Smith, Phys. Rev. 105, 1417 (1957).
15. Two of these events are due to Pevsner, Ritson, and Widgoff, MIT-Harvard private communication.
16. Chupp, Goldhaber, Goldhaber, and Webb, Interactions of Negative K Particles at Rest, UCRL-3044, June 1955; Nuovo cimento, Suppl. 4, 382 (1956).



17. Budde, Chrétien, Leitner, Samios, Schwartz, and Steinberger, Phys. Rev. 103, 1827 (1956).
18. Falla, Friedlander, Anderson, Greening, Limentani, Sechi-Zorn, Cernigoi, Iernetti, and Poiani, Nuovo cimento 5, 1203(1957); and Edward, Engler, Friedlander and Kamal, Nuovo cimento 5, 1188, 1957.
19. Fry, Schneps, Snow, Swami, and Wold, Phys. Rev. 104, 270 (1956):
20. Gilbert, Violet, and White, K-Particle Captures by Bound and Free Protons in Emulsion, UCRL-4814, Feb. 1957.
21. Cohen, Crowe, and Dumont, Phys. Rev. 104, 1266 (1956).
22. Barkas, Barrett, Cüer, Heckman, Smith, and Ticho, Phys. Rev. 102, 583 (1955);
- Relation in Emulsion*  
~~Preliminary Calculations: Range-Energy Curve for Protons in G.5 Emulsion of Density 3.815 g/cm<sup>3</sup> (High Velocity Portion), UCRL-3384, April 1956~~  
*3768 & UCRL-3769 to be published April 9, 1957*
23. Fry, Schneps, Snow, and Swami, Phys. Rev. 103, 226 (1956).
24. See for instance work by various emulsion groups in the Proceedings of the Fifth Annual Rochester Conference on High-Energy Physics, 1955 (Interscience, New York, 1955). Proceedings of the Sixth Annual Rochester Conference on High-Energy Physics, 1956, (Interscience, New York, 1956) and Proceedings of the Seventh Annual Rochester Conference on High-Energy Physics, 1957 (Interscience, New York, 1957).
25. We are assuming here that the  $K^- - \bar{K}^0$  mass difference is too small for charge exchange to occur for  $K^-$  interactions at rest with bound nucleons.
26. We have not included interactions leading to the production of two pions.
27. Francis H. Webb, Jr., I. The Interaction of Negative K Mesons at Rest in Complex Nuclei II. The  $K^-$  Mass,  $\Sigma^-$  Mass, and  $\Sigma^- - \Sigma^+$  Mass Difference (thesis), UCRL-3785, May 1957; A Similar Calculation was performed independently by Richard H. Capps, Optical Model of Sigma-Particle Production Nuclei by Negative K Mesons, UCRL-3707, March 1957.
28. Antiproton Collaboration Experiment, Phys. Rev. 105, 1037 (1957).
29. For the evaporation region we have assumed the same  $\alpha/p$  ratio and energy spectra for the  $\alpha$ 's and protons as has been observed in the  $\pi^-$  meson absorption stars; see Menon, Muirhead, and Rochat, Phil. Mag. 41, 583 (1950).

30. Edward E. Gross, The Absolute Yield of Low-Energy Neutrons from 190-Mev Proton Bombardment of Gold, Silver, Nickel, Aluminum, and Carbon (thesis), UCRL-3330, Feb. 1956.
31. Fry, Snow, Schneps, and Swami, Phys. Rev. 103, 226 (1956).
32. M. Bartlett, Phil. Mag. 44, 249 (1953).
33. Fry, Schneps, Snow, Swami, and Wold, Phys. Rev. 107, 257 (1957).
34. Glasser, Seeman, and Snow, Phys. Rev. 107, 277 (1957).
35. Frank, Gammel, and Watson, Phys. Rev. 101, 891 (1956).
36. Brueckner, Serber, and Watson, Phys. Rev. 84, 258 (1951).
37. Bernardini, Booth, and Lederman, Phys. Rev. 83, 1075 (1951);  
Bernardini, Booth, and Lederman, Phys. Rev. 83, 1277 (1951);  
G. Bernardini and F. Levy, Phys. Rev. 84, 610 (1951);  
G. Goldhaber and S. Goldhaber, Phys. Rev. 91, 467 (1953); and  
A.H. Morrish, Phys. Rev. 90, 674 (1953).